Geophysical surveys to help map buried igneous intrusions, Snowdonia, North Wales, UK

Moseley, D.P.[1,2], Pringle, J.K.[1]*, Haslam, R.B.[1,3], Egan, S.S.[1], Rogers, S.L.[1], Gertisser, R.[1], Cassidy, N.J.[1] & Stimpson, I.G.[1]

[1]School of Physical and Geographical Sciences, Keele University, Keele, Staffordshire, ST5 5BG, U.K.

[2]Hannon Westwood, 8 Old Lodge Place, St. Margaret's, Twickenham, Middlesex, TW1 1RQ, U.K.

[3]British Geological Survey, Environmental Science Centre, Nicker Hill, Keyworth, Nottingham, NG12 5GG, U.K.

*contact email: j.k.pringle@keele.ac.uk

Abstract

The geology of the Snowdonia National Park in North Wales comprises a mixture of Lower Palaeozoic shallow marine sediments, acidic igneous rocks and basic intrusions of the Welsh Basin that were subsequently deformed during the Caledonian Orogeny. Thin igneous intrusions are challenging to map due to variable surface exposures, their intrusive origin, structural deformation and burial by glacial sediments. This study used a combination of traditional geological techniques, near-surface geophysical surveys and remote sensing to detect and map a buried dolerite sheet intrusion. Both simple and mathematical analysis of magnetic anomalies and numerical modelling allowed the dolerite position, depths and target widths to be determined. Results showed that calibrated magnetic surveys can characterise buried igneous bodies in such mountainous environments.

Introduction

For geologists, standard field mapping of exposed geology and obtaining sedimentary and structural data is critical to provide a geological map, cross section and geological history of a field area. It is also important to map buried geology where exposures are more variable. Remote sensing imagery analysis can aid with this but often cannot provide high resolution of both the location the identification of buried geology.

Near-surface geophysical surveys can detect, characterise and estimate the depth of buried bedrock geology. Modern geophysical survey methods can also be rapidly undertaken and cover large areas in short time frames. Magnetic surveys have been very effective to map buried bedrock geology, provided there is a sufficient contrast in magnetic susceptibility between the target and background rocks. The overlying sediment deposits also need not to be too thick. Bulk ground electro-magnetic (EM) conductivity surveys can also map contrasting rock types and associated boundaries. Seismic surveys have been used to map buried bedrock depth but suffer from poor resolution and would be logistically difficult to collect in such environments. Ground Penetrating Radar (GPR) surveys suffer from limited penetration depths. Lastly, microgravity datasets have been used to map buried bedrock geology but need significant rock density contrasts and is difficult to acquire in mountainous terrain.

This paper shows how traditional geological mapping, remote sensing and near-surface geophysics can create a detailed map of partially buried geology in mountainous terrain in the Snowdonia National Park in North Wales (**Fig. 1**). This also included determining the extent of a dolerite sheet intruded into older sedimentary and acidic volcanic rocks, all of which were partially buried by glacial deposits. Near-surface geophysical surveys were also collected to test their suitability and effectiveness. Lastly, simple and numerical analysis and numerical modelling were combined to determine likely target depths and widths.

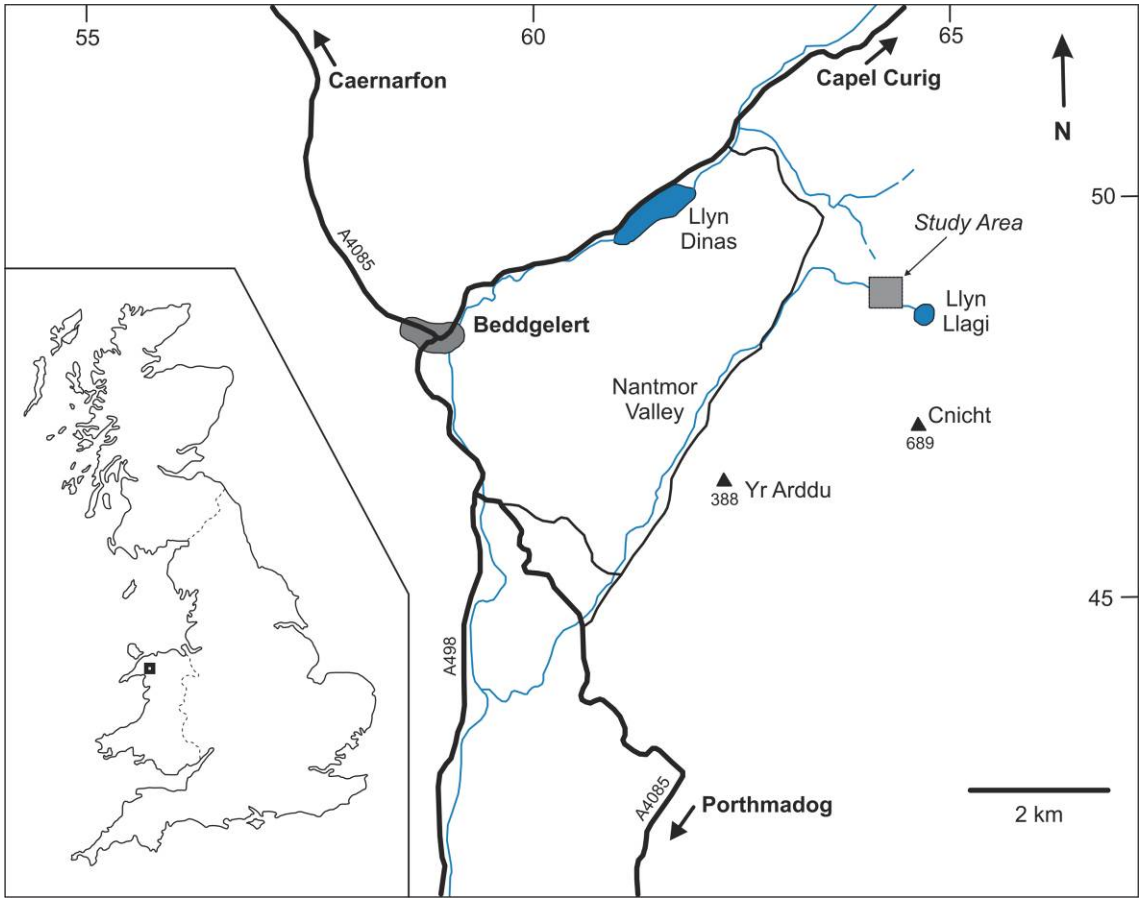

Fig. 1. Location map of the study area (boxed) with U.K. location map (inset).

Geological background

The geology of the Snowdonia National Park in North Wales comprises a thick sequence of Lower Palaeozoic shallow marine sediments, acidic igneous rocks and basic intrusions of the Welsh Basin. The sediments comprise mudstones, siltstones, sandstones and volcanic tuffs of both the Cwm Eigiau Formation and Nant Ffrancon Subgroup (**Fig. 2**) and typically contain mono-mineralic quartz assemblages (**Fig. 3A-C**). Igneous activity was associated with a marginal basin that developed on the Avalonia continental terrane as a result of subduction and closure of the Iapetus Ocean at ~450 Ma. Igneous activity is characterised by both basic and acidic igneous rocks, with the latter consisting of rhyolitic lavas and, in some cases, thin sheet-like intrusions, dominated by quartz and alkali feldspar (**Fig. 3D-F**), with volcaniclastic ignimbrites deposits (**Fig. 3G-I**). These igneous units are from the Lower Rhyolitic Tuff and Penmaen Tuff Formations (**Fig. 2**) of the Snowdon Volcanic Group. The rocks are cut by a number of later Ordovician sheet-like basic dolerite intrusions (**Fig. 2**), which consist of clinopyroxene, plagioclase feldspar and magnetite (**Fig. 3J-L**). Post-depositional Caledonian Orogeny tectonic processes led to widespread structural deformation. This major tectonic event developed cleavage, tectonic joints, regional low-grade (sub-greenschist) metamorphism and large-scale faulting and folding (*cf.* **Fig. 2**). Subsequent Quaternary glaciations have varied the quality and extent of rock outcrops (**Fig. 4**). Glacial deposition is primarily responsible for outcrop cover, burying the basic dolerite intrusion that forms a major geophysical target here.

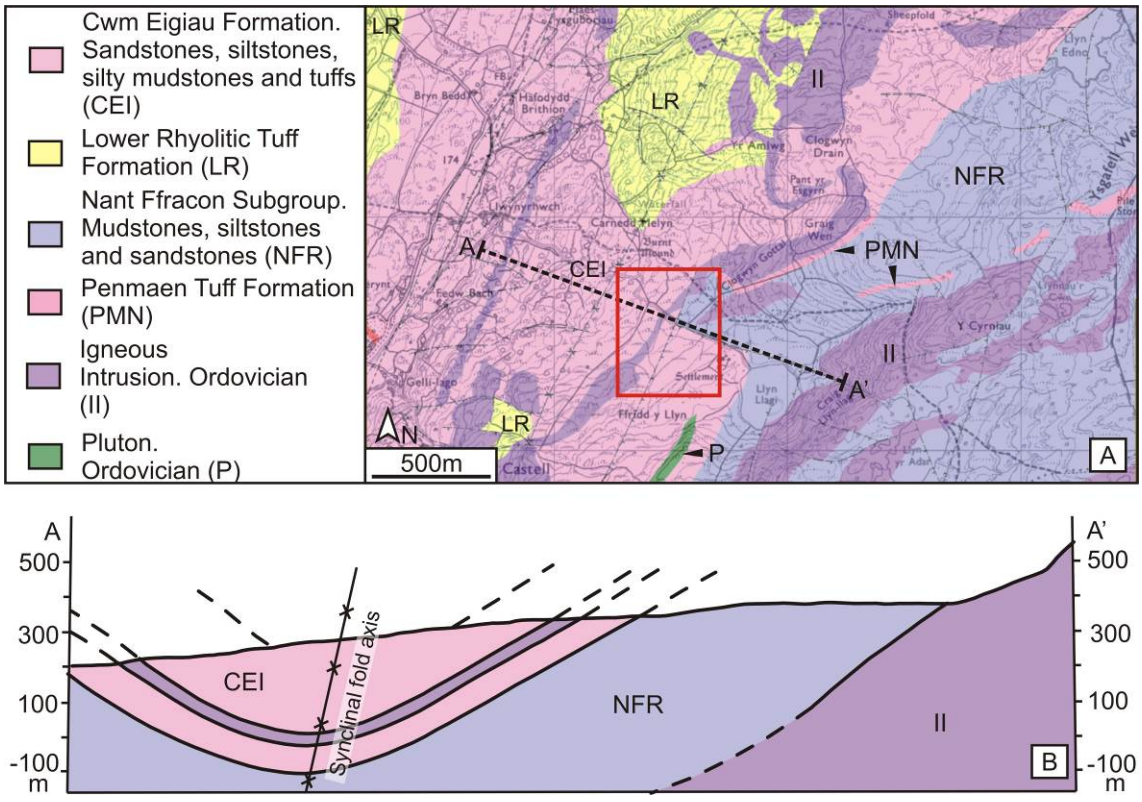

Fig 2. Geology of the southern Snowdonia area. (A) Local geology (see key) and study area (red box). (B) Schematic cross-section with position marked in (A). Modified from British Geological Survey (BGS) Sheet 119 (1997).

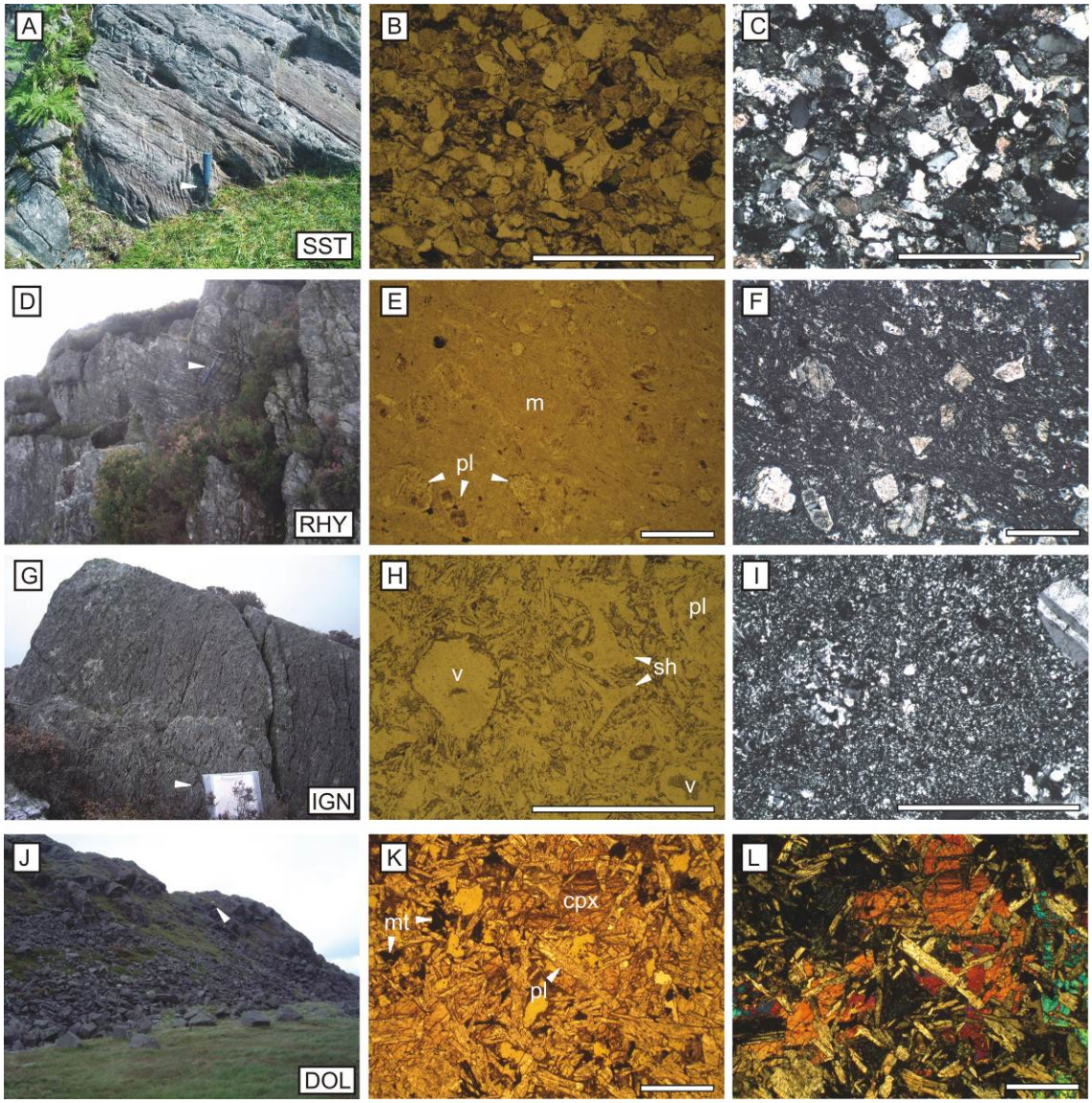

Fig. 3. Main rocks (left) with thin sections in plane-polarised (middle) and cross-polarised (right) light. (A-C) Medium-bedded quartz-rich sandstone; (D-F) Flow-banded rhyolite with phenocrysts (ph) of quartz and alkali feldspar in fine-grained matrix (m); (G-I) Devitrified acidic (rhyolitic) volcaniclastic ignimbrite deposits with characteristic eutaxitic texture (G). Thin sections show vesicles (v), y-shaped (originally glassy) bubble-wall fragments/shards (sh) and crystals of plagioclase feldspar (pl); (J-L) columnar-jointed dolerite containing plagioclase feldspar (pl), clinopyroxene (cpx) and magnetite (mt). Geological field hammers (arrows) for scale with thin section 1mm scale bars.

Methodology

The study area (**Figs. 2a** and **4**) was geologically mapped over 10 days, identifying and locating rock exposures and lithological boundaries, with major rock type hand specimens collected for thin section analysis (**Fig. 3**). Structural data, including cleavage, bedding and fault plane locations, were also obtained to allow the structural reconstruction of the area (**Fig. 2b**) and aid interpretations of geophysical datasets. To obtain magnetic susceptibility measurements of the main rock types, specimens were used to create ~1 cm^3 cylindrical 10g samples. Samples were placed within a Bartington™ MS2B calibrated (1%) dual frequency sensor and each measured 12 times to gain mean and error bounds (typically less than +/-2.5%).

Recent Quaternary sediments that overlay bedrock geology were a mixture of glacially-derived local erratic rocks up to 1 m in diameter and gravel-sized debris down to fine sands and silts. There was also a significant stream running west in the middle of the study area, sourced from Llyn Llagi, a lake to the southeast (**Fig. 4**), and was an obvious source of stream-derived sediments.

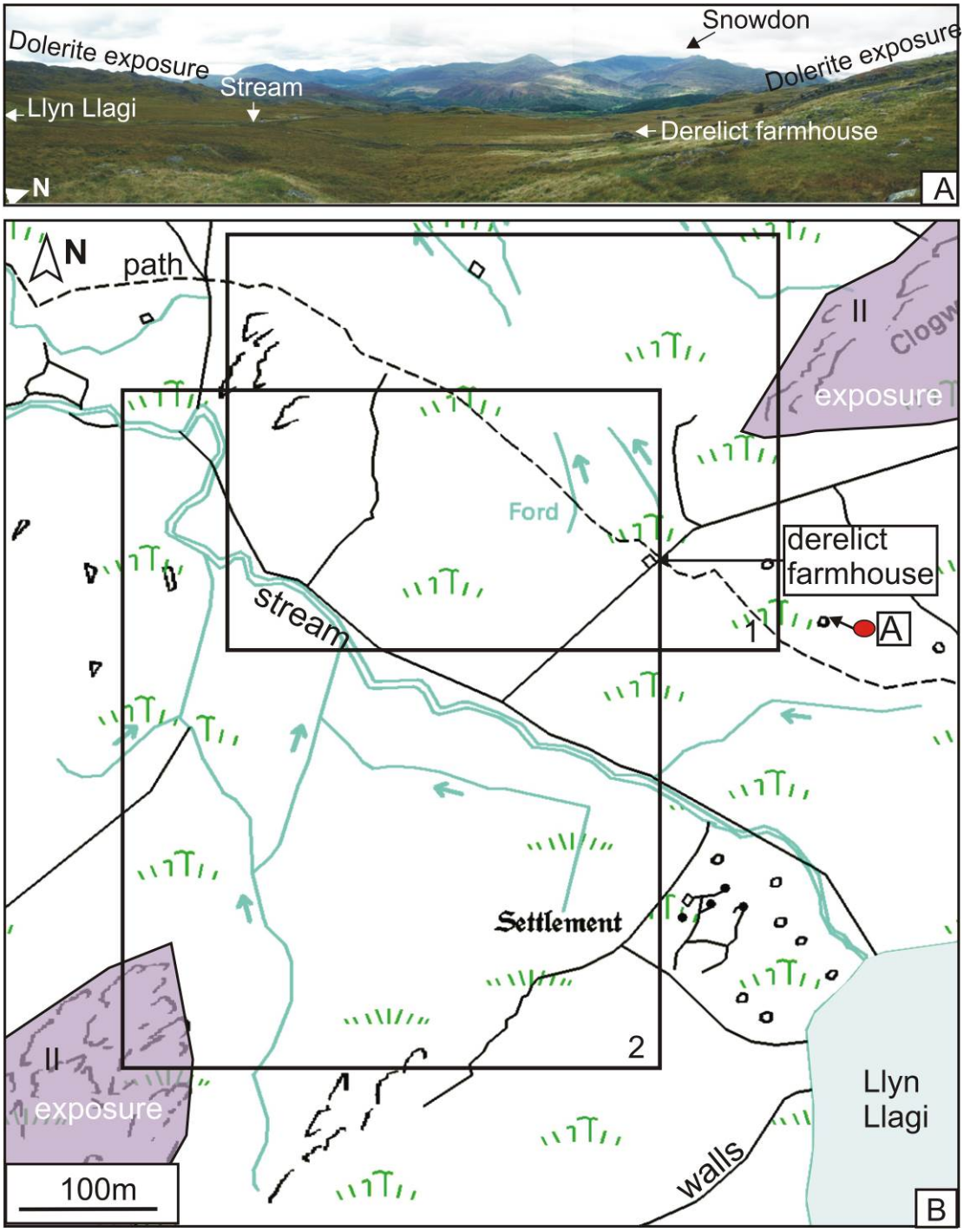

129

130 **Fig. 4.** (A) Photomosaic of study area (foreground) showing recent deposits

131 burying bedrock geology, with Snowdon in background. (B) Study areas

132 showing exposed outcrop and buried geology.

133

Digital aerial photographs of the survey area were ortho-rectified and digitally overlain onto topographic maps to identify outcrop positions, confirm any structural trends identified from ground mapping and recognise lineations not identified at outcrop. Potential buried outcrop locations were also recognised.

An Elsec™ 825 total field proton precession magnetometer collected fourteen 2D profiles over three days, using 10 m sampling spacing where possible. Each sample point had a minimum of three readings acquired, with up to five recorded if there was a large variability observed in the readings. 2D profiles were orientated perpendicular to the presumed dolerite, based on geological and remote sensing mapping data.

A Very Low Frequency (VLF) conductivity Geonics™ EM-16 receiver instrument with 24 KHz (Maine, US source transmitter) obtained local EM field vector angles at ~10 m spaced sample locations on the same 2D profiles. VLF data are not usually collected in the UK as the transmitter at Rugby has been switched off. For each sample position, the instrument was orientated first horizontally and then vertically to gain null positions sensed using an audio signal, before the vector angle was recorded. A second EM conductivity survey was collected using a Geonics™ EM-31 Mark-2 instrument, used in Vertical Magnetic Dipole mode and with GPS locationing. Both the inphase and apparent conductivity measurements were recorded at ~3 m intervals.

157 Magnetic and EM-31 datasets were processed by; (1) data 'de-spiking' to
158 remove anomalous data points using a ±2 SD filter; (2) diurnal correction
159 (magnetics); (3) detrending to remove long wavelength site effects; (4) profile
160 average adjustment to match cross-line measurements and; (5) importing into
161 software and linear gridding to best-fit a digital surface.

162

163 **Survey Results**

164

165 Geological field mapping located and identified the main rock types in the study
166 area. A spatially extensive but laterally thin dolerite intrusion was identified
167 intruding through older sedimentary units with a northeast-southwest trend;
168 however this could not be observed due to recent burial. Thin section analysis
169 showed the sandstone rocks contained well sorted mono-mineralic quartz
170 assemblages. In contrast, the dolerite intrusion consists of clinopyroxene,
171 plagioclase feldspar and, importantly, an iron-bearing mineral (magnetite). All
172 lithologies had the chlorite mineral present, consistent with regional, low-grade
173 metamorphism.

174

175 The rock sample magnetic susceptibility measurements ranged from 214.3 e^{-6} –
176 222.9 e^{-6} S.I. in the sandstone to 410.3 e^{-6} to 418.0 e^{-6} in the target dolerite,
177 indicating a geophysically mappable relative magnetic susceptibility contrast of
178 at least 200 e^{-6} S.I.

179

Aerial photograph interpretation identified several poorly exposed outcrops which were investigated. Structural interpretation identified several small faults that may have displaced the target dolerite intrusion. An extensive lineation to the southwest was interpreted to be a strike-slip fault orientated, supported by abundant field quartz mineralisation (**Fig. 5**). Several other interpreted faults corresponded to the regional northwest-southeast Caledonian trend.

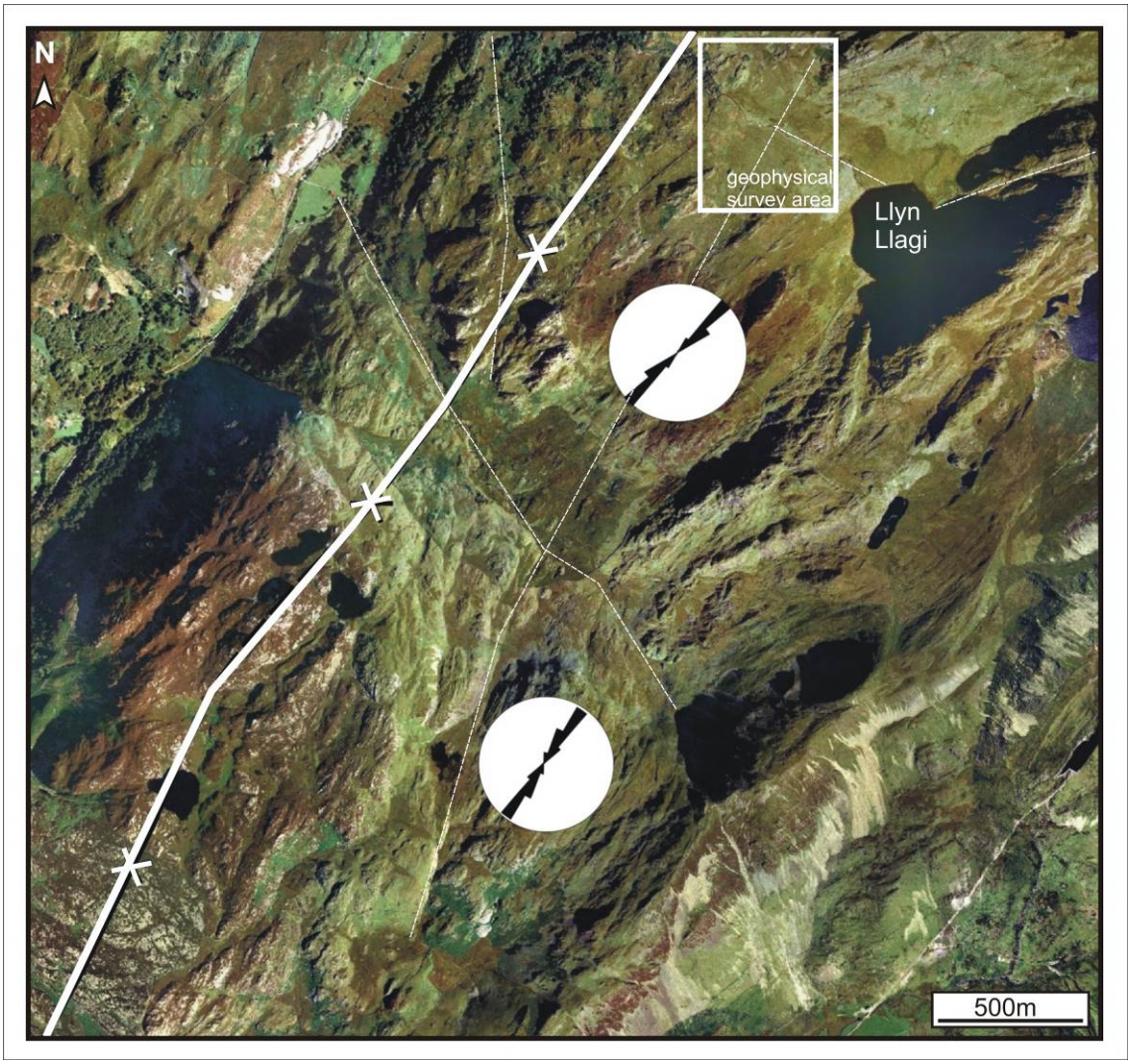

Fig. 5. Remote sensing image (study area marked), with interpreted faults (dotted lines) and summary structural trend rose diagrams. The major Yr Arddu structural syncline axis position also marked (white line).

The magnetic dataset had a well defined, northeast-southwest trending, area of relatively high magnetism, with respect to background values, in the centre of the study area (**Fig. 6a** and **7a**). Total field intensity measurements ranged from 49,140 nT to 49, 210 nT. Determining the overlying drift deposits' thickness was difficult as anomaly amplitudes were variable between profiles, ~ 4 nT to ~ 60 nT higher than background.

The VLF vector field dataset showed overall high vector positive angles to the north and extreme south and relatively low vector negative angles to the south-central part of the study area (**Fig. 6b**). This suggests that the conductivity anomaly was orientated east-west. Qualitative analysis of 0º dip angle locations on 2D profiles, commonly used in VLF surveys to indicate target positions, did not show an obvious correlation between profiles (**Figs. 6b** and **7b**). The apparent conductivity EM-31 inphase dataset showed a general area of high conductivity in the centre of the study area (**Fig. 6c**). The EM-31 quadrature dataset showed a fairly well-defined, northeast-southwest aligned area of high conductivity located in the centre (**Figs. 6d** and **7c**). EM-31 apparent conductivity quadrature values ranged from 0.38 mS/m to 6.5 mS/m with the highest recorded values located towards the north.

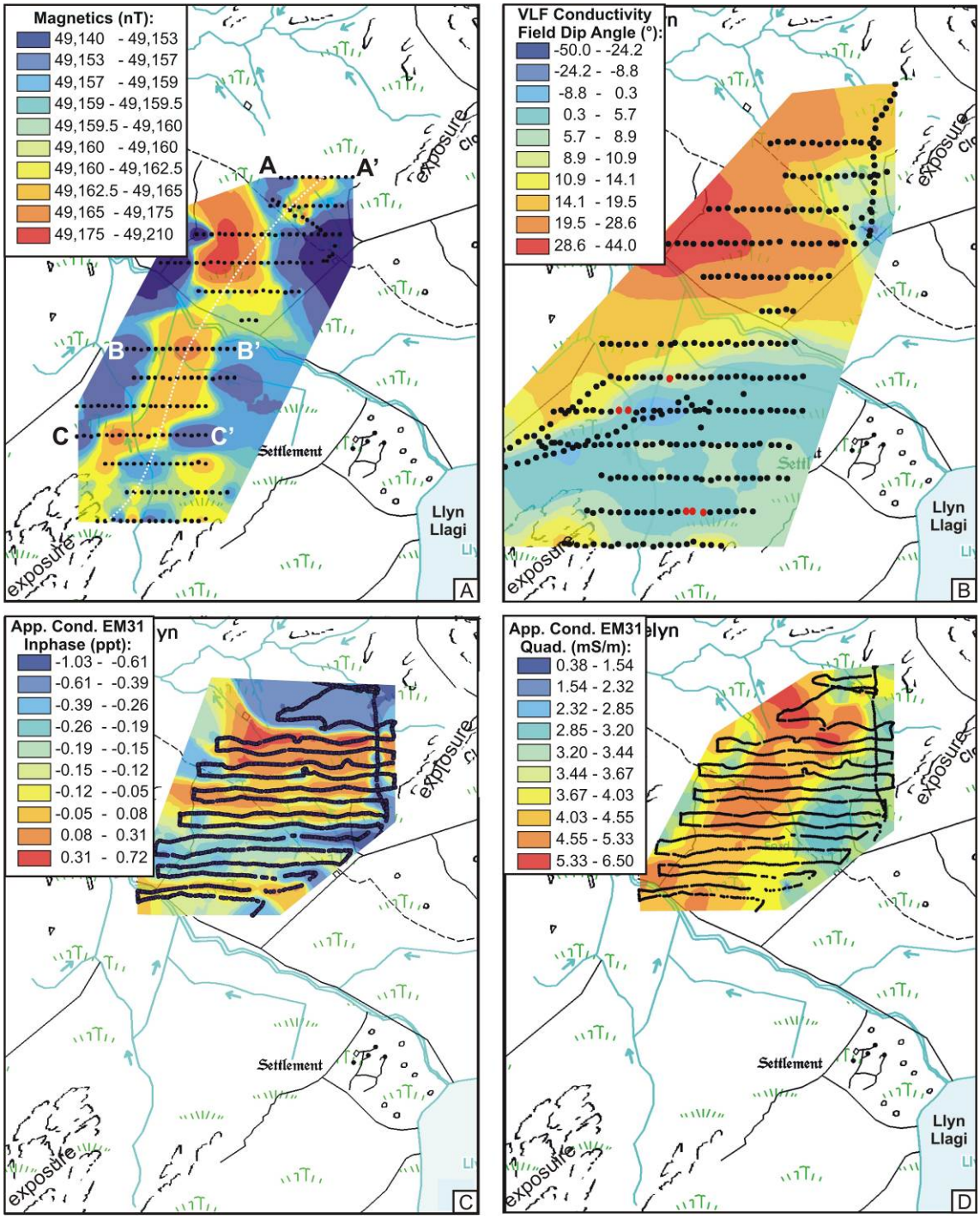

211

212 **Fig. 6.** (A-D) Colour contoured (see respective keys) geophysical maps of total
213 field magnetic, VLF and bulk ground conductivity EM-31 surveys. Black dots
214 are sampling positions. B – B' shows Fig. 7 geophysical profile. In (C) red dots
215 indicate 0º VLF field vectors.

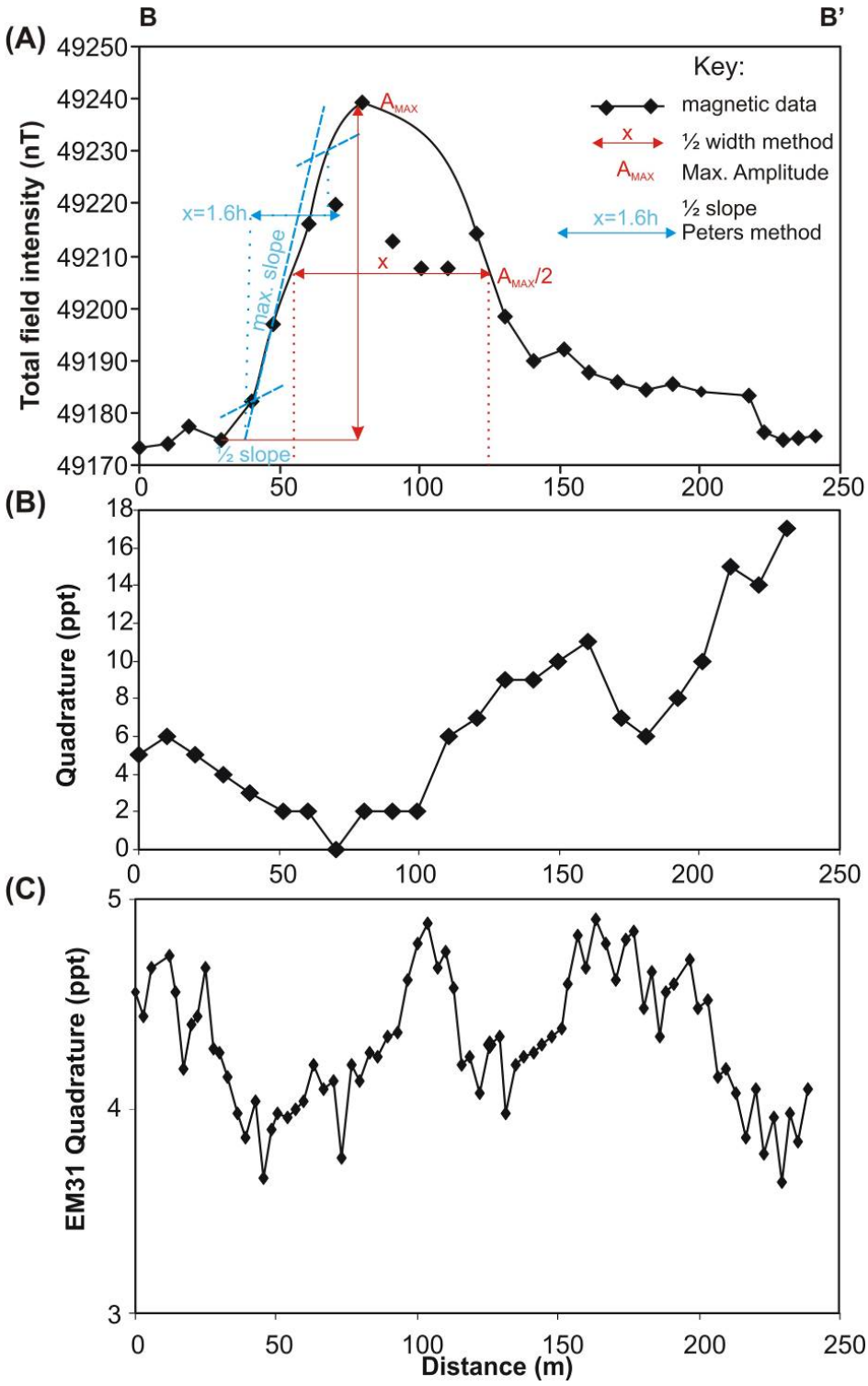

Fig. 7. 2D profile B comparison of geophysical data (Fig. 6B for location); (A) magnetics; (B) VLF and (C) EM-31 bulk ground surveys. (A) graphically illustrates target depth ½ width (red) and Peters half-slope (blue) estimation methods; calculated depths of ~35 m and ~65 m on this profile.

Target depth estimation

Simple graphical analysis of geophysical anomaly relative shapes and amplitudes can be used to determine target depth(s) and orientation(s). The half-width and Peters half-slope methods were used on magnetic profiles (see **Fig. 7A**); but target depth estimates were quite variable, between ~7 m to ~75 m on eleven of the fourteen profiles. The half-width method does not work when the target is not symmetrical or vertical; therefore the half-slope method was used to calculated target depths, generating a NE-SW trending transect across the study area (**Fig. 8**). Whilst useful, these target depth estimation methods can have a 30% measurement error with depths in the centre also being quite variable.

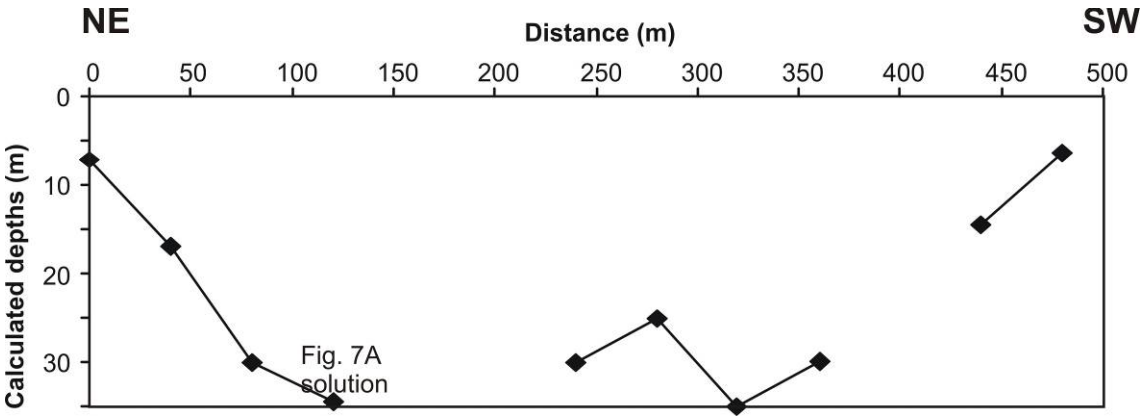

Fig. 8. Calculated target depths transect across the study area (Fig. 6B for location). These solutions based on Peters' ½ slope method on 2D magnetic profile anomalies (Fig.7A solution marked).

239 Euler deconvolution provides numerical solutions for bodies causing
240 geophysical anomaly relative shapes and amplitudes using a structural index.
241 2D magnetic profile data were analysed using this method using structural index
242 1, a vertical tabular body best estimating the target. This is quantitative,
243 corrects for the Earth's magnetic field and gives clusters of structural solutions
244 and target depths (**Fig. 9a**). Euler deconvolution depth solutions varied from 2
245 m – 27 m with a 10 m average across the study area, their spatial positions
246 merged into a single dataset to create a best-fit digitally contoured surface.
247 This (**Fig. 9b**) showed a similar trend to Peters' ½ slope method calculations but
248 were less variable and generally shallower. The deepest target depth mirrored
249 both the orientation of the stream and a local fault (*c.f.* Figs. 5 and 9b).
250

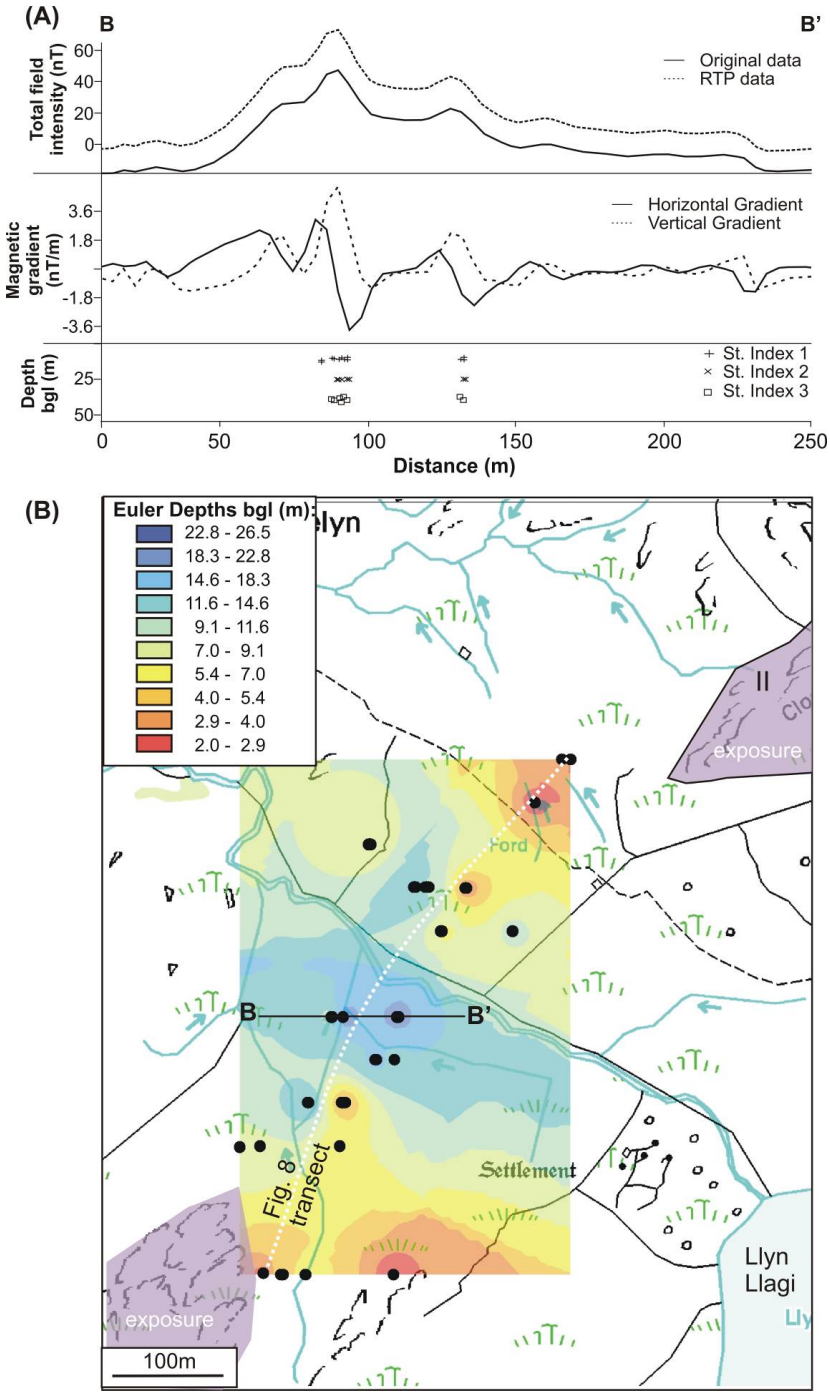

Fig. 9. (A) Euler deconvolution on 2D magnetic profile B (Fig. 6B for location). (top) original data and reduced to magnetic pole (RTP); (middle) horizontal and vertical gradient and (bottom) euler deconvolution solution for structural indices 1-3 (see text). (B) Colour contoured bedrock depth using euler deconvolution structural index 1 solutions (black dots).

2D Numerical modelling

Numerical modelling can determine buried target(s) depths and widths by creating models of buried layer(s) and/or object(s) with geometries and relative values. A calculated magnetic profile can be generated by combining modelled body values, also adjusting for local geophysical fields and profile orientations. The calculated profile can then be quantitatively compared with field-collected data; any resulting mis-fit can be analysed and reduced by either changing the modelled body values and/or modelled body geometries and spatial positioning.

2D depth models were generated for twelve profiles using geology information, rock sample magnetic susceptibility measurements and Euler deconvolution solutions. These profiles were calibrated to observed data and misfits reduced by only varying target intrusion body width and drift geology body geometries (**Fig. 10**). Model mis-fits were small (12.7 to 67.5 with a 33.5 average), which gave confidence that models were reasonable. The modelled target dolerite width was variable (10 – 60 m with a 28.6 m average), with two intrusions needing to be modelled in the south. Spatial positions of modelled target intrusions were transferred onto a study site map, together with Euler deconvolution solution locations for comparison (**Fig. 11**).

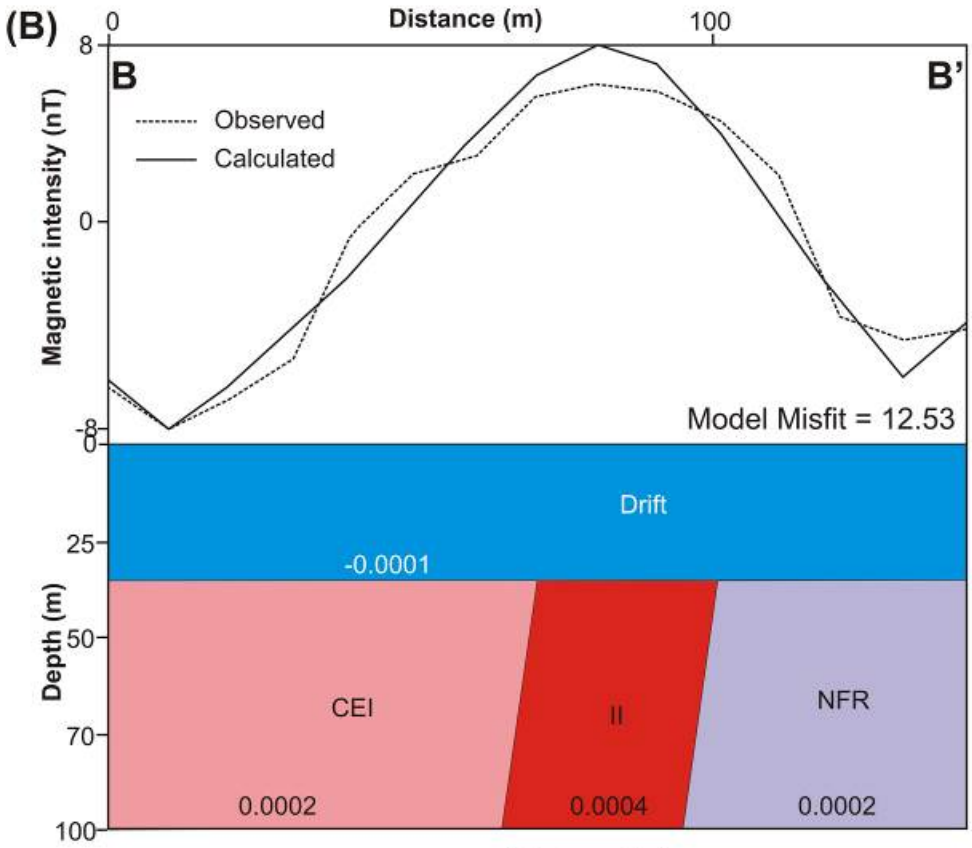

277

278 **Fig. 10.** 2D magnetic numerical model of profile B (position in Fig. 6B). (top)
279 Observed and model-calculated magnetic data and (bottom) 2D model with rock
280 (Fig.2 for key) body geometries and magnetic susceptibility values.

281

282 **Discussion**

283

284 The use of geological mapping combined with remote sensing can construct
285 basic geological maps of a study area. Ground-based near-surface geophysics,
286 particularly magnetics, can detect buried highly ferromagnetic geological
287 targets, based on higher magnetic and bulk ground conductivity values.
288 Laboratory magnetic susceptibility measurements of field rock samples also

289 gave confidence in geophysical findings. Qualitative analysis of the EM VLF
290 dataset showed an approximately east-west orientated feature correlated with a
291 suspected fault zone. Magnetic surveys were good quality and analysed using
292 simple graphical methods of 2D magnetic profiles. Euler deconvolution
293 solutions gave more quantitative target depths that showed a similar geometry
294 transect but were less variable and significantly shallower (averages of ~10 m
295 for Euler versus ~23 m for Peters half-slope method respectively). Numerical
296 modelling created models calibrated by outcrop and remote sensing, magnetic
297 profile field data, rock sample magnetic susceptibility measurements and Euler
298 deconvolution solutions. Relatively small mis-fits between model-calculated
299 magnetic profiles and collected magnetic datasets were generated by
300 numerically varying the target body width and superficial deposit thicknesses..

301

302 Combining all datasets allowed an accurate geological map to be created (**Fig.**
303 **11b**), which would not have been possible without integration of near-surface
304 geophysical datasets, and their detailed analysis described in this study. The
305 magnetic survey was deemed crucial to not only locate and map the target
306 igneous intrusion, but also to allow depth estimates to be quantitatively
307 estimated. This detailed analysis went beyond conventional survey
308 methodologies and also allowed the location of later structural displacements,
309 namely linear strike-slip faults with typical Caledonian Orogeny orientations, to
310 be suggested to best-fit the datasets.

311

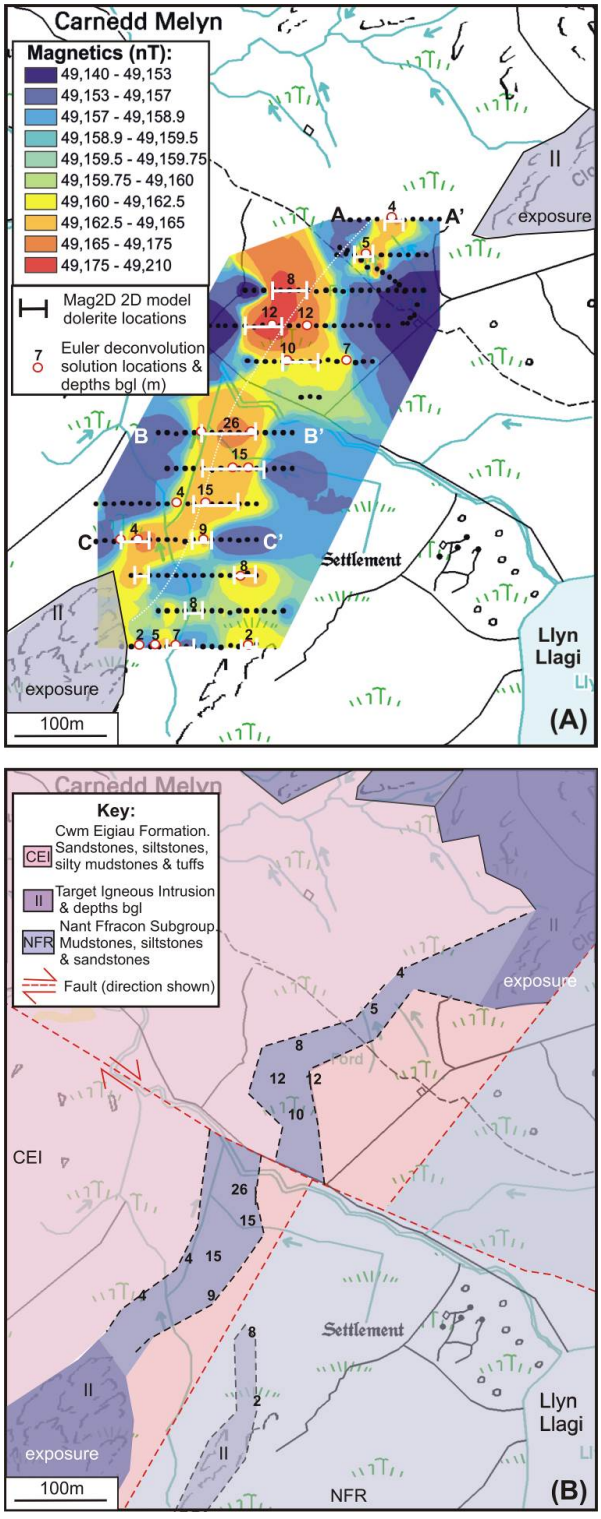

312

313 **Fig. 11.** (A) Summary map of target dolerite intrusion from numerical models.

314 Fig. 6B contoured magnetic data underlayed. Euler deconvolution locations

315 and calculated depths also shown. (B) Summary map, numbers indicating

316 target depths and with a offsetting fault present.

Conclusions

Detailed geological mapping, remote sensing and near-surface geophysics were all combined to generate a detailed geological map. Total field magnetometer surveys were critical in determining a buried target dolerite sheet intrusion. The EM VLF technique detected a east-west orientated conductive structural feature. Simple graphical analysis of magnetic anomalies was shown to delineate bedrock depth but quantitative Euler deconvolution solutions of magnetic anomalies were most accurate which was, on average, ~13 m shallower than graphical analysis results. Finally 2D numerical modelling confirmed the depth of overburden. The final geological map generated agrees with the generally agreed geological evolution of the area.

Further reading:

Howells M.F. and Smith M. 1997. *Geology of the country around Snowdon. The Stationery Office*, London.

Lisle R., Brabham P. and Barnes J. 2011. *Basic Geological Mapping. The Geological Field Guide Series*, John Wiley and Sons Ltd., 5th Edition.

Milsom J. and Eriksen A. 2011. *Field Geophysics*. The Geological Field Guide Series: 4th Edition. Wiley.

338 Murdie R.E., Styles P., Upton P., Eardley P. and Cassidy N.J. 1999. Euler
339 deconvolution methods used to determine the depth to archaeological features.
340 In: Pollard A.M. (ed.) Geoarchaeology: exploration, environments, resources.
341 *Geological Society of London Special Publication* **165**, 35-40.

342 Pringle J.K., Cassidy N.J., Styles P., Stimpson I.G. and Toon S.M. 2010.
343 Training the next generation of near-surface geophysicists: team-based
344 student-led, problem-solving field exercises, Cumbria, U.K. *Near Surface*
345 *Geophysics* **8**, 503-517.

346 Reynolds J.M. 2011. *An Introduction to Applied and Environmental Geophysics*.
347 2nd Edition. Wiley.

348 Schofield D. 2009. What's in the Welsh Basin?: insights into the evolution of
349 Central Wales and the Welsh Borderlands during the Lower Palaeozoic.
350 *Proceedings of the Shropshire Geological Society* **14**, 1-17.